University of Exeter

UK Research and Innovation

Phytoplankton Response to Climate Change (PRIME)

Simulating vertical phytoplankton dynamics in a stratified ocean using a two-layered ecosystem model

Author(s): Qi Zheng, Johannes J. Viljoen, Xuerong Sun, Žarko Kovac, Shubha Sathyendranath and Robert J.W. Brewin

1. Background

Phytoplankton are responsible for most of the transfer of carbon dioxide from the atmosphere to the ocean and contribute nearly half of Earth's primary production.

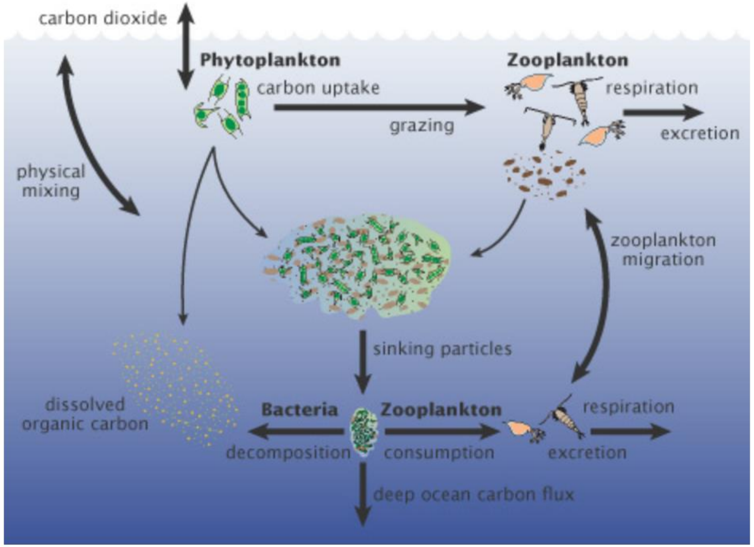

Fig 1: Carbon cycle in oceans modulated by phytoplankton

University of Exeter

1. Background

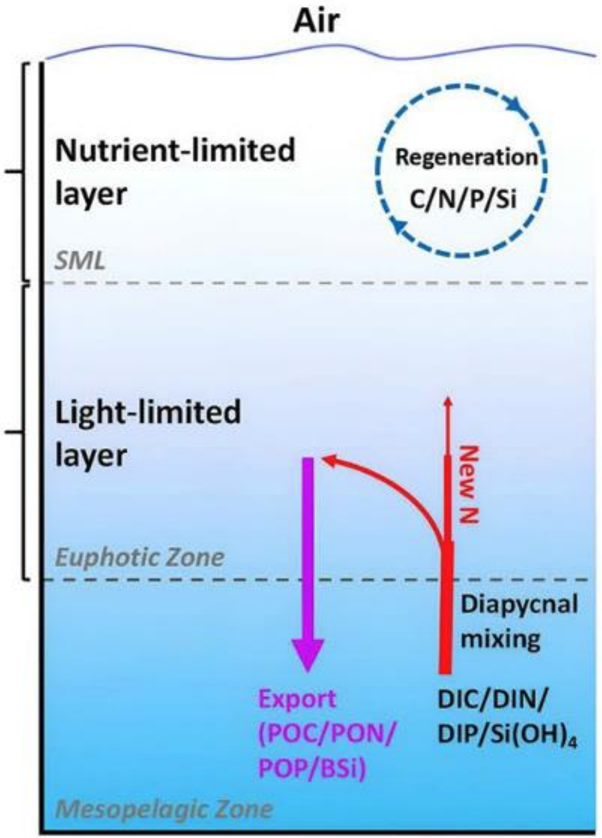

Fig 2: The two-layered structure of upper ocean biogeochemistry in oligotrophic gyres from Dai et al. (2023). The surface mixed layer (SML) divides the euphotic zone into the upper nutrient-limited layer and the lower light-limited layer.

Around 70% of the ocean is characterised by either seasonal or permanent stratification.

Considering the potential expansion of stratified waters with climate change, it is crucial to better understand their phytoplankton dynamics.

1. Background

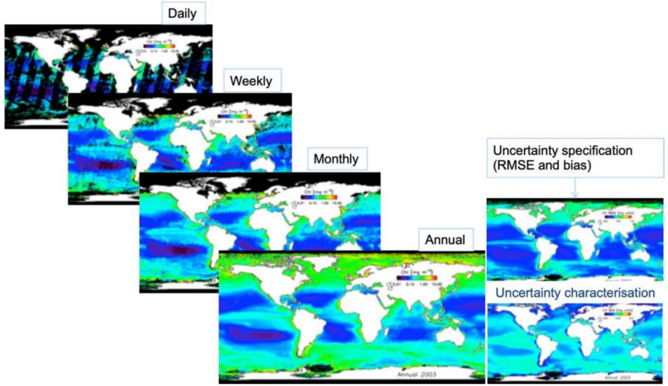

Fig 3: Some examples of chlorophyll products from ocean colour climate change initiative.

We usually rely on satellite remote sensing of ocean colour.

In stratified oceans, there's a deeper, less understood phytoplankton community that satellites can't observe.

This community can contribute a substantial portion of the total water-column phytoplankton biomass and can have contrasting phenology to surface communities.

University of Exeter

1. Background

Viljoen et al. (2024) observed a decreasing trend in chlorophyll integration within the Mixed Layer Depth (MLD) but an increasing trend between the base of the mixed layer and euphotic zone at Bermuda Atlantic Time-series Study (BATS; a stratified ocean) from 2011 to 2022.

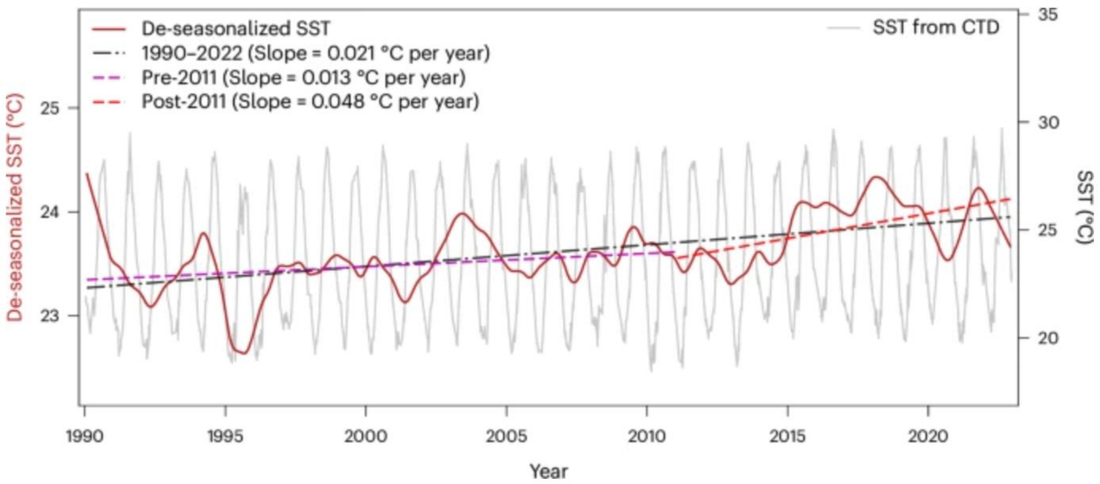

Fig 4: Multidecadal increasing surface-ocean temperature trend from Bermuda Atlantic Time-series Study (BATS) and how it changed over the last 12 years.

University of Exeter

2. Aim:

To understand the mechanisms driving contrasting trends of phytoplankton above and below the mixed layer depth from 2011 to 2022.

1. To develop a two-layered ecosystem box model.

2. To run the model at Bermuda (31°S) and compare model outputs with observations. We develop the C:Chl-a ratio (following Jackson et al. (2017)) to convert the unit of nitrogen (mmol m^{-2}) to chlorophyll (mg m^{-2}) in this model.

3. To identify the drivers of the observed trends.

Fig 5: A map showing the location of Bermuda.

University of Exeter

3.1 Method:

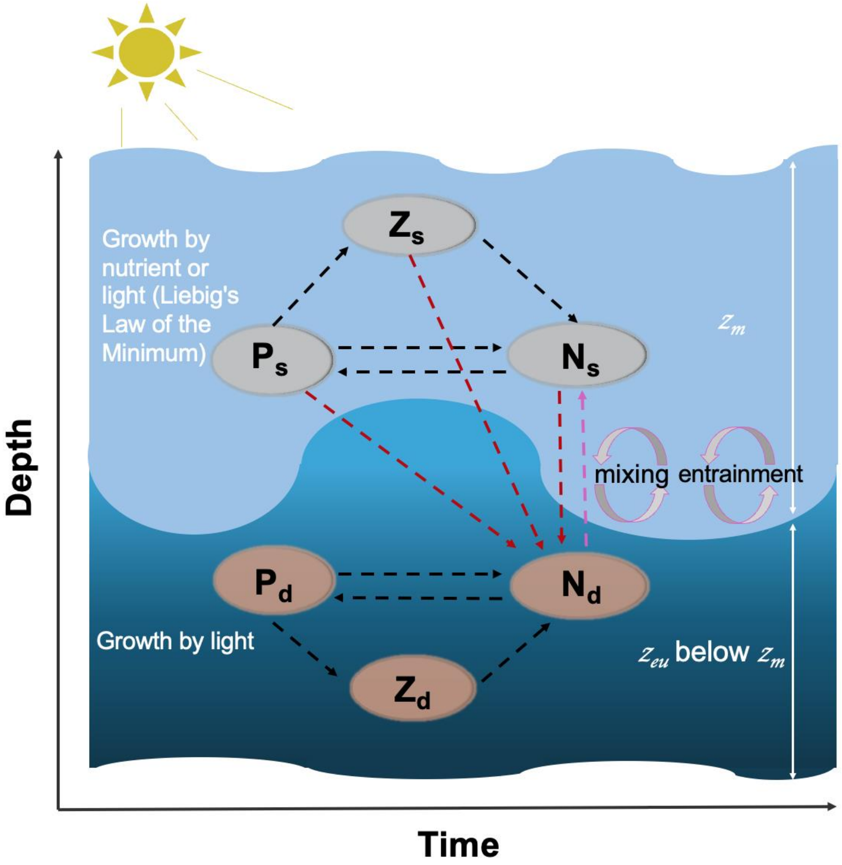

Fig 6: Schematic diagram of the two-layered ecosystem model. Light and dark blue shades represent the surface and subsurface layers respectively. P_s , Z_s and N_s (P_d , Z_d and N_d) refer to the phytoplankton, zooplankton and nutrient pools at the surface (subsurface) respectively. z_m and z_{eu} refer to mixed layer depth and euphotic zone respectively. Following Miller and Wheeler (2012) and Brock (1981), we model daily averaged solar radiation at BATS site assuming clear sky conditions

3.3 Method: model parameters

Table 1. Parameters used in our two-layered NPZ model, their meanings, values, units and supporting references.

Parameter	Symbol	Value	Unit	Reference
Solar constant	$SolarK$	1373	Wm^{-2}	Miller and Wheeler (2012)
Atmospheric attenuation	Atm	0.5	—	Miller and Wheeler (2012)
PAR fraction	f_{par}	0.41	—	Fasham et al. (1990)
Light attenuation due to water	K_{dw}	0.04	m^{-1}	Fasham et al. (1990)
Surface chlorophyll-specific light attenuation coefficient	K_{dp_s}	0.028	$m^2(mgChla)^{-1}$	Uitz et al. (2008)
Initial value for surface nutrient concentration	N_o	0.1	$mmolNm^{-3}$	Anugerahanti et al. (2020)
Initial value for nutrient concentration in the subsurface layer	N_{d_o}	2.5	$mmolNm^{-3}$	Anugerahanti et al. (2020)
Initial value for phytoplankton concentration at the surface	P_o	0.2	$mmolNm^{-3}$	Kantha (2004)
Initial value for zooplankton concentration at the surface	Z_o	0.25	$mmolNm^{-3}$	Anugerahanti et al. (2020)
Initial value for chlorophyll concentration at the surface	Chl_o	0.1	mgm^{-3}	Anugerahanti et al. (2020)
Initial value for phytoplankton concentration at the subsurface	P_{d_o}	0.1	$mmolNm^{-3}$	Doney et al. (1996)
Initial value for zooplankton concentration at the subsurface	Z_{d_o}	0.05	$mmolNm^{-3}$	Anugerahanti et al. (2020)
Initial value for chlorophyll concentration at the subsurface	Chl_{d_o}	0.13	mgm^{-3}	Anugerahanti et al. (2020)
Initial value for mixed layer depth	z_{m_o}	52	m	Time-mean z_m at BATS
Initial value for euphotic zone	z_{e_o}	250	m	Anugerahanti et al. (2020)
Half-saturated for phytoplankton nutrient uptake at surface layer	K_s	0.7	$mmolNm^{-3}$	Hurtt and Armstrong (1999)
Initial slope of the P/I curve at surface layer	α_s	0.025	$day^{-1}(Wm^{-2})^{-1}$	Fasham et al. (1990)
Phytoplankton mortality rate at surface layer	m_s	0.09	day^{-1}	Fasham et al. (1990)
Phytoplankton maximum growth rate at surface layer	V_{max_s}	1.2	day^{-1}	Schartau and Oschlies (2003)
Zooplankton assimilation efficiency at surface layer	γ_s	0.75	—	Fasham et al. (1990)
Maximum grazing rate at surface layer	a_s	2	day^{-1}	Oschlies and Garçon (1999)
Prey capture rate at surface layer	ϵ_s	1	$(mmolNm^{-3})^{-2}day^{-1}$	Oschlies and Garçon (1999)
Zooplankton quadratic mortality rate	c_s	0.2	$(mmolNm^{-3})^{-1}day^{-1}$	Pasquero et al. (2005)
Dead zooplankton fraction immediately available as nutrient	μ_z	0.2	—	Pasquero et al. (2005)
Zooplankton grazing substance fraction sinking to the subsurface layer	μ_g	0.2	—	Pasquero et al. (2005)
Dead phytoplankton fraction immediately available as nutrient	μ_p	0.2	—	Pasquero et al. (2005)
Mixing fraction coefficient	μ_m	0.0055	—	Fennel et al. (2001)
Subsurface chlorophyll-specific light attenuation coefficient	K_{dp_d}	0.026	$m^2(mgChla)^{-1}$	Uitz et al. (2008)
Initial slope of the P/I curve at subsurface layer	α_d	0.256	$day^{-1}(Wm^{-2})^{-1}$	Schartau and Oschlies (2003)
Phytoplankton mortality rate at subsurface layer	m_d	0.05	day^{-1}	Schartau and Oschlies (2003)
Phytoplankton maximum growth rate at subsurface layer	V_{max_d}	0.27	day^{-1}	Schartau and Oschlies (2003)
Zooplankton assimilation efficiency at subsurface layer	γ_d	0.9	—	Schartau and Oschlies (2003)
Maximum grazing rate at subsurface layer	a_d	1.575	day^{-1}	Schartau and Oschlies (2003)
Prey capture rate at subsurface layer	ϵ_d	1.6	$(mmolNm^{-3})^{-2}day^{-1}$	Schartau and Oschlies (2003)
Zooplankton quadratic mortality rate at subsurface layer	c_d	0.34	$(mmolNm^{-3})^{-1}day^{-1}$	Schartau and Oschlies (2003)
Maximum chlorophyll-to-carbon ratio at surface layer	θ_m	0.01	$gChlagC^{-1}$	Jackson et al. (2017)
C:N Redfield ratio for phytoplankton	$Q_{C:N}$	$\frac{106}{16}$	$mmolC(mmolN)^{-1}$	Redfield (1958)
Molecular weight of Carbon	M_c	12	$mgC(mmolC)^{-1}$	—
C:Chl ratio at subsurface layer	χ_d	156	—	Half of the modelled time-mean C:Chl ratio at surface layer

Parameters, their meanings, values, units and supporting references.

4.1 Results:

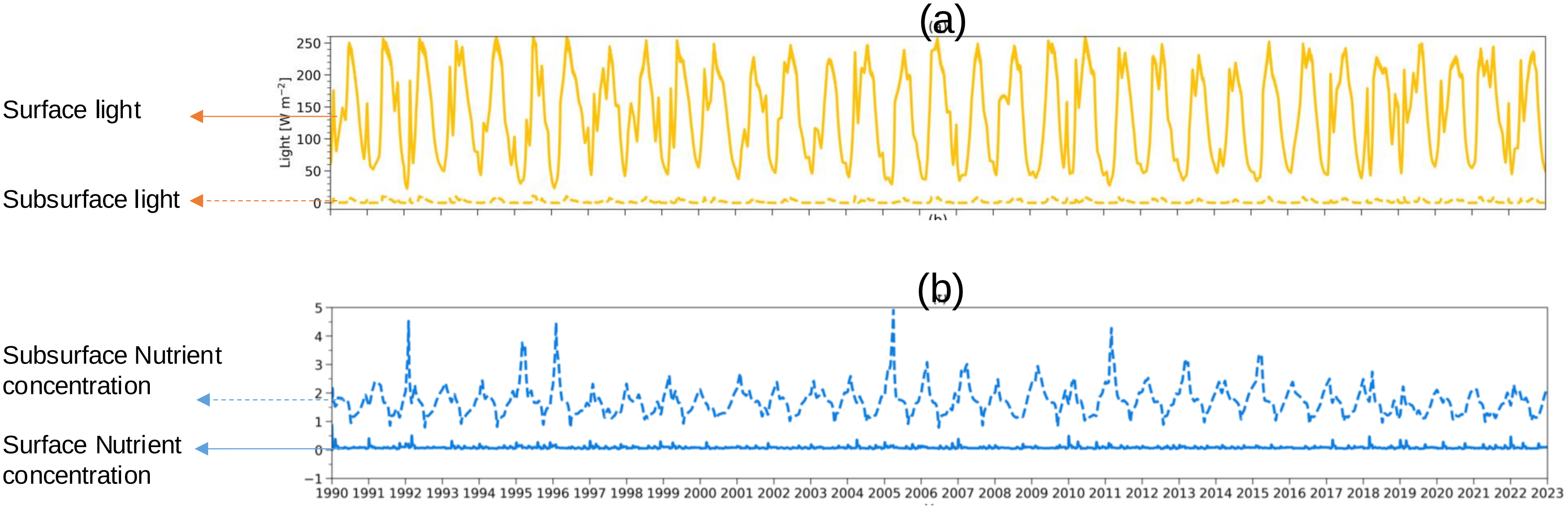

Fig 7: Light (yellow) and nutrient concentration (blue) at two layer running from the two-layered model

4.2 Results: full signal and seasonality

Corr. = 0.77

Corr.= 0.31

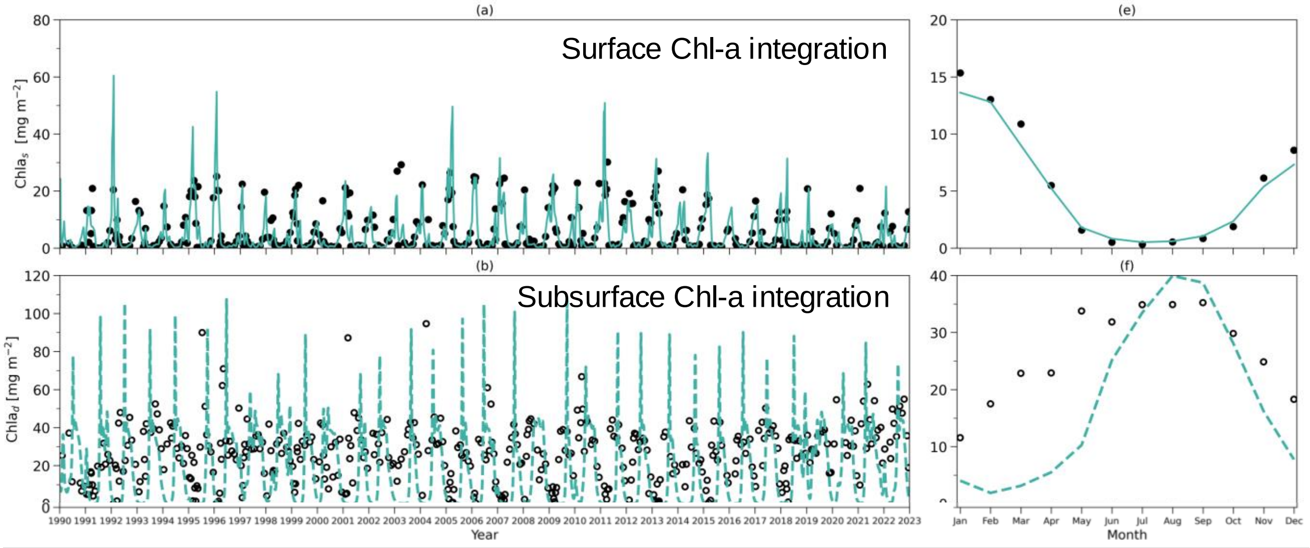

Fig 8: Chl-a vertical integration from model (green lines) and **observations (black dots)** at the BATS site

4.3 Results: interannual variability

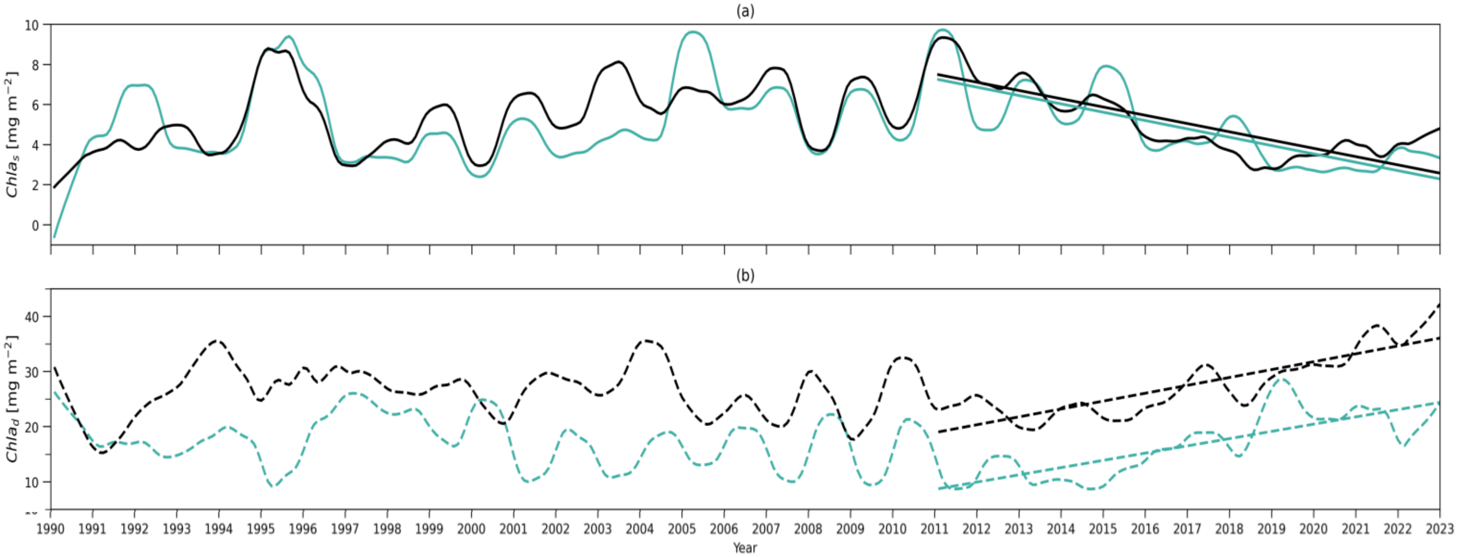

Corr. (post 2011) = 0.85

Corr. (post 2011) = 0.75

Fig 9: Interannual variability of Chl-a vertical integration from model (green) and **observations (black)** at BATS.

University of Exeter

4.3 Results: mechanism

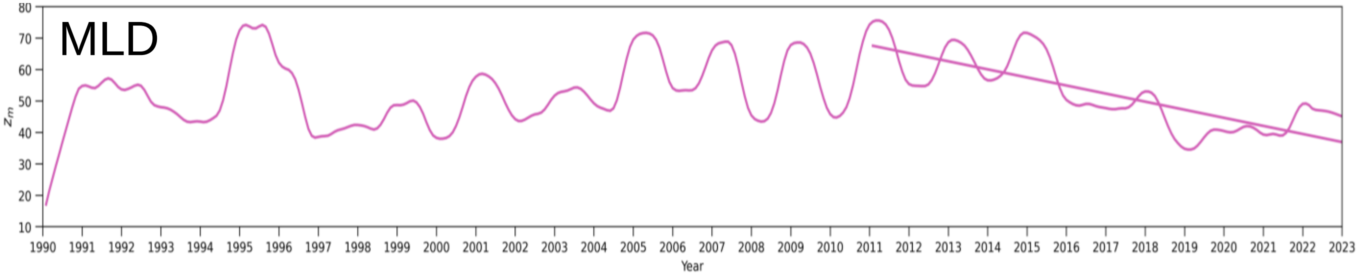

Fig 10: Interannual variability of observational MLD (pink line).

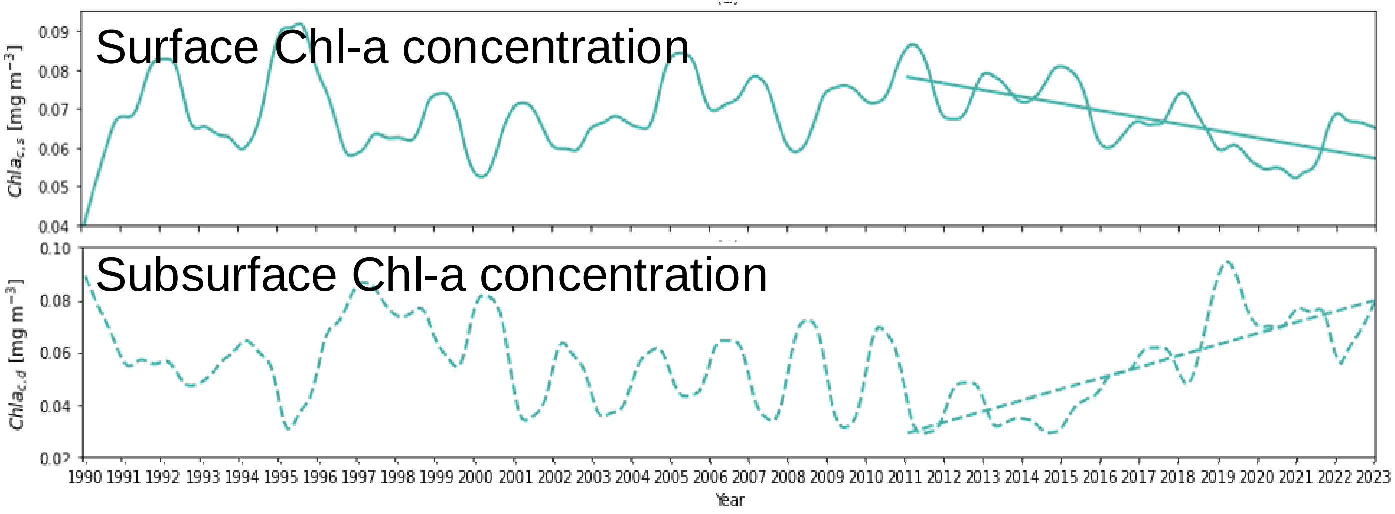

Fig 11: Interannual variability of Chl-a vertically averaged concentration from model (green).

4.3 Results: surface mechanism

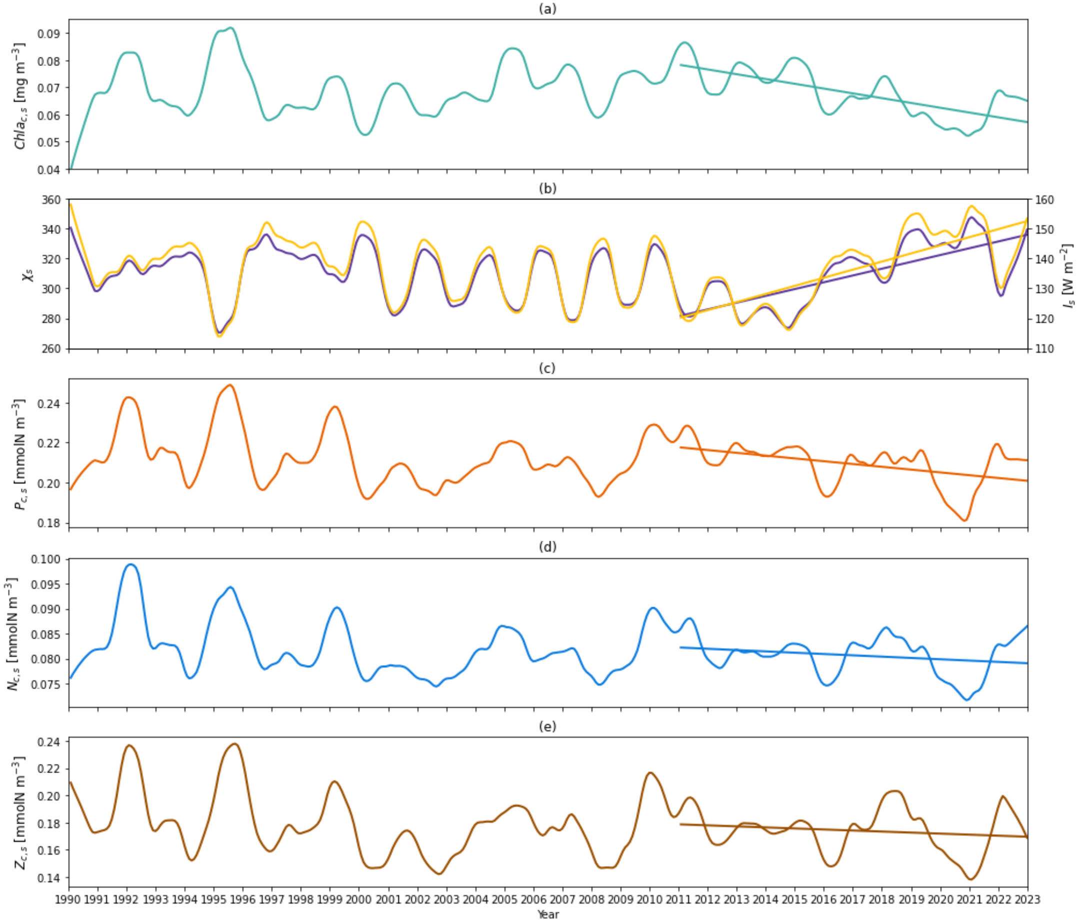

Chl-a concentration

S = - 0.002 *mg m^{-3} yr^{-1}*
Δ = - 27 %

Light & C:Chl-a ratio

S = 2.71 *Wm^{-2} yr^{-1}*
Δ = 27 %
S = 4.54 *yr^{-1}*
Δ = 19 %

P_s concentration

S = - 0.001 *mmol m^{-3} yr^{-1}*
Δ = - 8 %

N_s concentration

S = 0
Δ = - 4 %

Z_s concentration

S = *not significant*
Δ = - 5%

4.3 Results: subsurface mechanism

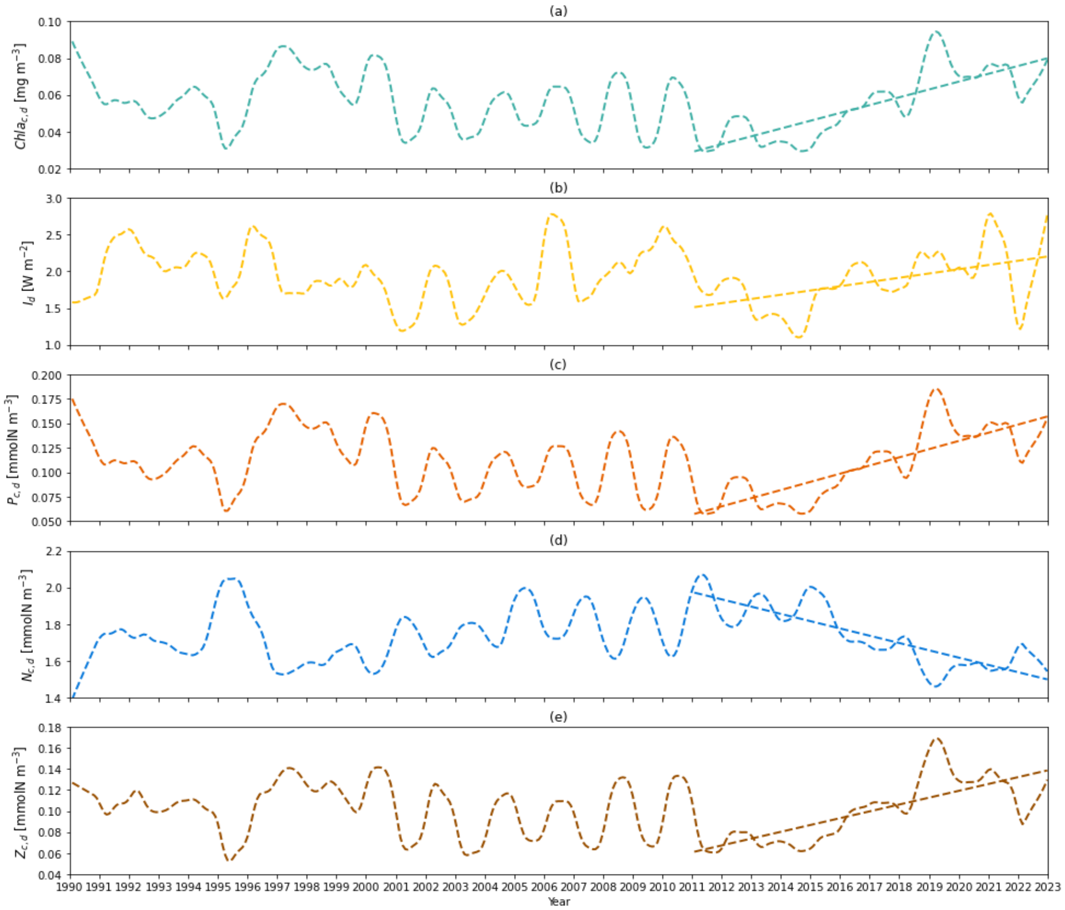

Chl-a concentration

S = 0.004 $mg\ m^{-3}\ yr^{-1}$
Δ = + 172 %

Light

S = 0.058 $Wm^{-2}\ yr^{-1}$
Δ = + 45.5 %

P_d concentration

S = + 0.008 $mmol\ m^{-3}\ yr^{-1}$
Δ = + 172 %

N_d concentration

S = - 0.040 $mmol\ m^{-3}\ yr^{-1}$
Δ = - 24 %

Z_d concentration

S = + 0.006 $mmol\ m^{-3}\ yr^{-1}$
Δ = + 126 %

5. Take-home messages

- We developed a two-layer NPZ model for stratified oceans, partitioning the euphotic zone into two layers.

- This model simulates the chlorophyll seasonal and interannual variability at two layers, reproducing observed contrasting trends in chlorophyll between two layers over 2011-2022.

- Mechanism:

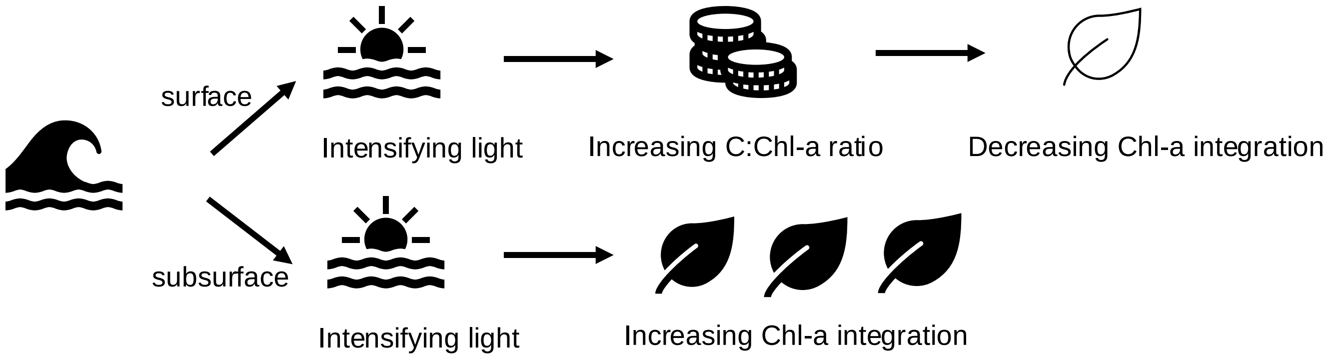

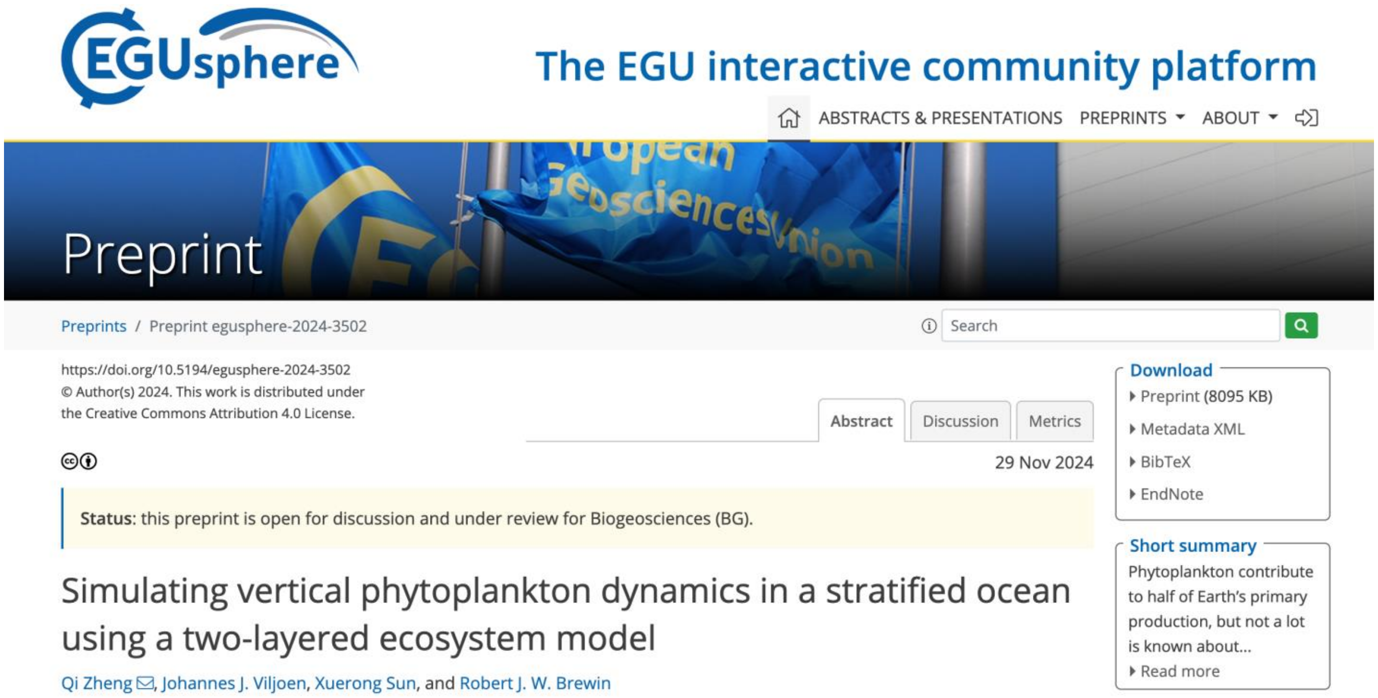

University of Exeter

Dai, M., Luo, Y.W., Achterberg, E.P., Browning, T.J., Cai, Y., Cao, Z., Chai, F., Chen, B., Church, M.J., Ci, D. and Du, C., 2023. Upper ocean biogeochemistry of the oligotrophic North Pacific Subtropical Gyre: from nutrient sources to carbon export. *Reviews of Geophysics*, *61*(3), p.e2022RG000800.

Viljoen, J.J., Sun, X. & Brewin, R.J.W. 2024. Climate variability shifts the vertical structure of phytoplankton in the Sargasso Sea. *Nat. Clim. Chang.* 14, 1292–1298. https://doi.org/10.1038/s41558-024-02136-6

Thank you!
Q&A